J Mol Model (2005) 12: 85–92
DOI 10.1007/s00894-005-0009-7

ORIGINAL PAPER

Carlos Ramero · Patricia Guadarrama · Serguei Fomine

Interactions in pseudorotoxanes based on crown ether-secondary ammonium motifs. A theoretical study

Received: 16 February 2005 / Accepted: 29 June 2005 / Published online: 28 October 2005

Abstract A theoretical analysis of the nature of the interactions in dibenzo[24]crown-8 (DB24C8)-*n*-dibutylammonium (DBM)—pseudorotaxane complex at the MP2 and DFT levels shows that the main contribution to the binding energy is the electrostatic interaction with moderate (20–25%) correlation stabilization. The total binding energy in the DB24C8-DBM complex represents a sum of the binding energies of two NH–O and one CH–O hydrogen bonds and the latter constitutes about 25% of the total interaction energy, giving the total binding energy of −41.2 kcal mol^{-1} at the BHandHLYP/6-311++G** level. Deprotonation of the DB24C8-DBM complex reduces the binding energy by some 50 kcal mol^{-1}, giving metastable complexes DB24C8-DBA-1 or DB24C8-DBA-2, which will dissociate to give free crown ether and *n*-dibutylamine because of the strong exchange repulsion that prevails in neutral complexes.

Keywords Molecular switch · Dibenzo[24]crown-8 · Dibutylammonium · MP2 · DFT

Introduction

It is well known that crown ethers can form complexes with RNH_3^+ ions [1–3]. The chemical consequences of this kind of interaction have been observed in many important processes like molecular recognition events [4], resembling some important biological processes like protein-transport across membranes [5], as well as producing binding sites for Lewis-basic ligands in artificial receptors [6, 7]. More recently, it has been shown that suitably chosen $R_2NH_2^+$ ions can thread through the cavities of appropriately constituted crown ethers to give inclusion complexes with pseudorotaxane-like geometries [8, 9]. Interactions between crown ethers and $R_1R_2NH_2^+$ ions were used in the design of systems of both photochemical and photophysical interest. Their structural features have been studied by X-ray crystallography in the solid state, ^1H NMR spectroscopy in solution and mass spectrometry in the gas phase [10]. Investigations of the molecular recognition between a crown ether of at least the [24]crown-8 constitution and an NH_2^+ center on a threaded dialkylammonium ion have led to the realization that such systems could serve as a basis for pH-controllable molecular shuttles in situations involving competitive multiple recognition sites. Indeed, such an ''all-or-nothing'' molecular switch was described [11] in the literature in 1997. It involves DB24C8 as the ring component and a 4,4′-bipyridinium unit as the competing recognition site, also containing a NH_2^+ center for binding the crown ethers.

An example of an acid—base controllable molecular shuttle in which the rotaxane bears a fluorescent and redox-active anthracene stopper unit in addition to a dialkylammonium center and a bipyridinium unit has been reported by Stoddart et al. [12]. Upon addition of an appropriate base, the NH_2^+ group is deprotonated and the crown ether switches from the NH center to the bipyridinium. Treatment with acid restores the NH_2^+ center and reverses the process. Using the anthracene stopper, it is possible to monitor the switching process by means of electrochemical and photophysical techniques due to its absorption, luminescence, and redox properties.

It is believed that the interaction between an NH_2^+ center and a crown ether is essentially electrostatic in nature since the stability constant associated with the threading of $R_2NH_2^+$ ion decreases with the solvent polarity [13]. Similar conclusions have been reached in the studies of $C_6H_{11}NH_3^+$-18-crown-6 complex dissociation [14]. Close contact is observed between both NH protons and oxygen atoms located in the polyether's macrocycle. Additionally, one of the CH_2 protons in

C. Ramero · P. Guadarrama · S. Fomine (✉)
Instituto de Investigaciones en Materiales, Universidad Nacional Autónoma de México, Apartado Postal 70-360, CU, Coyoacán, 04510, México, México
E-mail: fomine@servidor.unam.mx

each methylene group linked directly to the ammonium center is within hydrogen-bonding distance, suggesting C–H–O interactions [13]. However, it has not been documented on a theoretical level that electrostatic interactions dominate crown ether–ammonium complexes.

Although there is some theoretical work on ammonium–crown complexes [15–18] it is limited to DFT or HF studies of crown–ammonium complexes. To the best of our knowledge, there is only one quantum-mechanical semiempirical study of a molecular complex between a secondary ammonium cation and DB24C8, which represents a model of a real molecular switch. The authors studied the process of switching between neutral and protonated states of this complex and although the semiempirical model predicts correctly the most important features of the switching process, this model is too simple to give a deep insight into the nature of intermolecular interactions [19]. Another approach [20] was used to understand the nature of interaction in paraquat-based catenanes and rotaxanes. In this work, a small model system consisting of methylpyridinium ion and dimethylether representing a model for the interaction between paraquat cycle and a polyethyleneoxide chain was used. The model system was studied at the MP2/6-311 + + G** level and the importance of CH–O hydrogen bonds between the charged system and oxyethylene chain was shown.

This work is an attempt to combine these two approaches. On one hand to use a model as close as possible to the real system, and on the other to use correlated ab initio and DFT methods to study the nature of intermolecular interactions in DB24C8-secondary ammonium-based pseudorotoxanes.

Computational details

The model system used for the calculations represents a complex of DB24C8 with the di-*n*-butylammonium cation as the charged species and DB24C8 with di-*n*-butylamine as the deprotonated one (Fig. 1). Because of the flexibility of the DB24C8 cycle, there are multiple local minima for these complexes. To get as close as possible to the global minimum, a conformational search was carried out for the charged complex using a Monte Carlo algorithm in combination with the MMF94 force field available in the Titan program [21]. The lowest energy structure was used for all further optimizations. A similar procedure was used for DB24C8 and the di-*n*-butylammonium cation. The initial structures for the neutral complex were generated by the elimination of one of the protons from the ab initio optimized structure of the charged complex, suggesting that deprotonation occurs faster than conformational changes.

It is important to select an appropriate theoretical method that offers a reasonable balance between computational cost and precision. To select this method, preliminary calculations were carried out on "models" of the model system; a complex of di-*n*-propylammonium and di-*n*-propylamine with dimethylether (DME). To study the nature of CH–O interactions, a model complex of tetramethylammonium (TMA) with DME was used as a model. First, the geometry was optimized at the MP2/6-31 + G* level and zero-point energy correction was determined. Then, the geometry was optimized at the MP2/6-311 + + G** level and binding energies were calculated taking into account basis set superposition error (BSSE) according to Ref. [22]. For comparison purposes, similar calculations were carried out at HF, B3LYP and BHandHLYP levels. The solvent effect on the binding energy was studied at the BHandHLYP level with the Poisson–Boltzmann method [23, 24] implemented in the Jaguar 5.5 suite of programs [25], which represents one of the modifications of the continuum model. All DFT geometry optimizations were carried out using the Jaguar 5.5 suite of programs. Single point energy evaluations at DFT and MP2 levels as well as MP2 geometry optimizations were carried out with the Gaussian 03 code [26]. The largest possible basis set (6-311 + + G**) was used for all calculations to reduce the effect of the basis set on the calculation results. Thus, all geometry optimizations and frequency calculations for DB24C8-containing complexes involved around 1,300 basis functions.

The Kitaura–Morokuma energy decomposition analysis [27] was carried out with the GAMESS program [28].

Results and discussion

Complexes of (DME) with *n*-dipropylamine (DPA), *n*-dipropylammonium (DPM) and TMA with DME as model systems for DB24C8-secondary ammomium-based

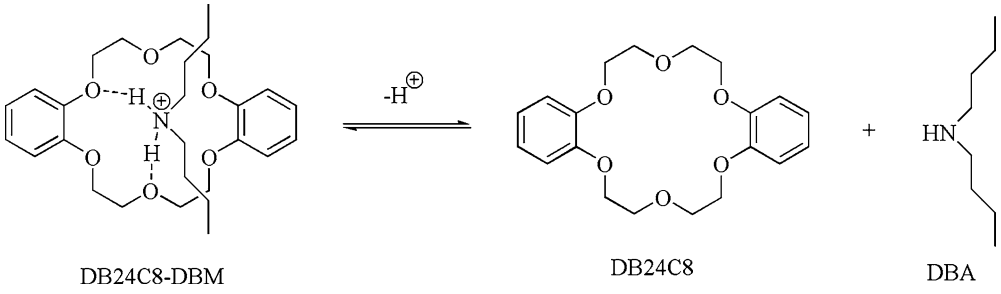

Fig. 1 Formation of DB24C8–DBM pseudorotoxane complex

Table 1 BSSE corrected gas phase binding energies (kcal mol^{-1}) at different levels of theory with ZPE corrections at 6-31 + G* level

MP2/6-311 + + G**			
Complex	MP2/6-311 + + G**	HF/6-311 + + G**	E_{corr}
DPA–DME	−2.76	0.55	−3.31
DPM–DME	−16.00	−12.25	−3.75
TMA–DME	−10.50	−7.36	−3.14
B3LYP/6-311 + + G**			
DPA–DME	−2.56		
DPM–DME	−15.26		
TMA–DME	−9.24		
BHandHLYP/6-311 + + G**			
DPA–DME	−2.77		
DPM–DME	−15.48		
TMA–DME	−9.21		
HF/6-311 + + G**			
DPA–DME	−1.76		
DPM–DME	−13.74		
TMA–DME	−8.18		
BHandHLYP/6-311 + + G**			
DB24C8–DBM	−41.2 (−30.21)[a]		
DB24C8–DBA−1	11.86		
DB24C8–DBA−2	11.78		
MP2/6-311 + + G**//BHandHLYP/6-311 + + G**			
	MP2/6-311 + + G**	HF/6-311 + + G**	E_{corr}
DB24C8–DBM	−43.60	−33.96	−9.64
DB24C8–DBA−1	7.67	20.33	−12.66
DB24C8–DBA−2	7.92	21.15	−13.23

[a]The free Gibbs binding energy at 298 K

pseudorotoxanes were studied at four different theoretical levels in order to find a compromise between accuracy and computational efficiency. The MP2 level of theory was chosen as a reference. As seen from Table 1, the binding energies of DPA–DME and DPM–DME complexes are very similar for MP2 and all DFT models, while the HF binding energies are less negative. When analyzing Table 1 one can see that underbinding at the HF level is related to ignoring the correlation stabilization, which reaches 3–4 kcal mol^{-1} for DPA–DME and DPM–DME complexes. The experimentally observed dissociation enthalpy for the dimethylammonium–water complex in the gas phase is 15 kcal mol^{-1} [29], very close to the binding energy obtained by the MP2 and DFT methods. A similar situation holds for the TMA–DME complex, where correlation stabilization represents about 20% of the total stabilization energy. The experimental data available for the TMA–water complex give a dissociation enthalpy of 9 kcal mol^{-1} [29], close to those obtained by DFT and MP2. The HF model, as seen from Table 1, slightly underestimates the stability of the CH–O ionic hydrogen bond. There is a big difference between the stabilization energies of charged (DPM–DME) and neutral (DPA–DME) complexes, which is the driving force for the switching process in pH-switchable molecular shuttles (Table 1). As seen in the case of neutral complex DPA–DME, the binding energy is completely due to correlation stabilization and the HF/6-311 + + G** stabilization energy is positive for MP2/6-311 + + G** optimized geometries. It is interesting to note that the correlation stabilization is similar for both charged and neutral complexes. However, the total stabilization energies for DPM–DME and DPA–DME are of −16.00 and −2.76 kcal mol^{-1}, respectively. The electrostatic, charge transfer and polarization contributions are responsible for the difference in binding energy between DPM–DME and DPA–DME complexes, as follows from the Kitaura–Morokuma energy-decomposition analysis.

Table 2 shows the Kitaura–Morokuma energy-decomposition of the HF interaction energy for

Table 2 The Kitaura–Morokuma Hartree–Fock interaction energy decomposition at HF/6-31G**//MP2//6-311 + + G** (m) and HF/6-31G**//BHandHLYP/6-311 + + G** (t) level of theory (kcal mol^{-1})

Complex	ES[a]	EX[b]	PL[c]	CT[d]	MIX[e]	HF[f]
DPA–DME (m)	−5.12	5.89	−0.48	−2.18	−0.25	−2.14
DPM–DME (m)	−23.48	18.86	−5.96	−6.11	0.12	−16.58
DB24C8–DPM (t)	−58.98	33.00	−14.07	−12.27	0.24	−52.09
DB24C8–DPA-1 (t)	−8.25	24.13	−1.79	−7.92	−0.01	6.15
DB24C8–DPA-2 (t)	−9.94	25.44	−1.90	−8.62	−0.23	4.74
TMA–DME (m)	−11.35	5.92	−2.15	−2.60	−0.06	−10.23

[a]Electrostatic energy
[b]Exchange repulsion energy
[c]Polarization energy
[d]Charge transfer energy
[e]High-order coupling energy
[f]Hartree–Fock energy

DPM–DME and DPA–DME complexes. As seen, the charge transfer, polarization and especially electrostatic interactions contribute most to the stabilization of the DPM–DME complex. The exchange repulsion originating from the electron repulsion on overlapped molecular orbitals is the most important destabilizing factor for the complexes. The strongest exchange repulsion is observed for the tight DPM–DME complex. Figure 2 shows selected geometrical parameters of the optimized structures of the DPM–DME, DPA–DME and TMA–DME complexes. It is noteworthy that the B3LYP- and HF-optimized geometries differ significantly from the MP2 and BHandHLYP geometries. Thus, the O–H distance in the DPA–DME complex optimized at the B3LYP and HF levels differs by 0.15 and 0.31 Å from those optimized at the MP2 level of theory. Such a big difference is due to the fact that DPA–DME complex stability is mostly related to the

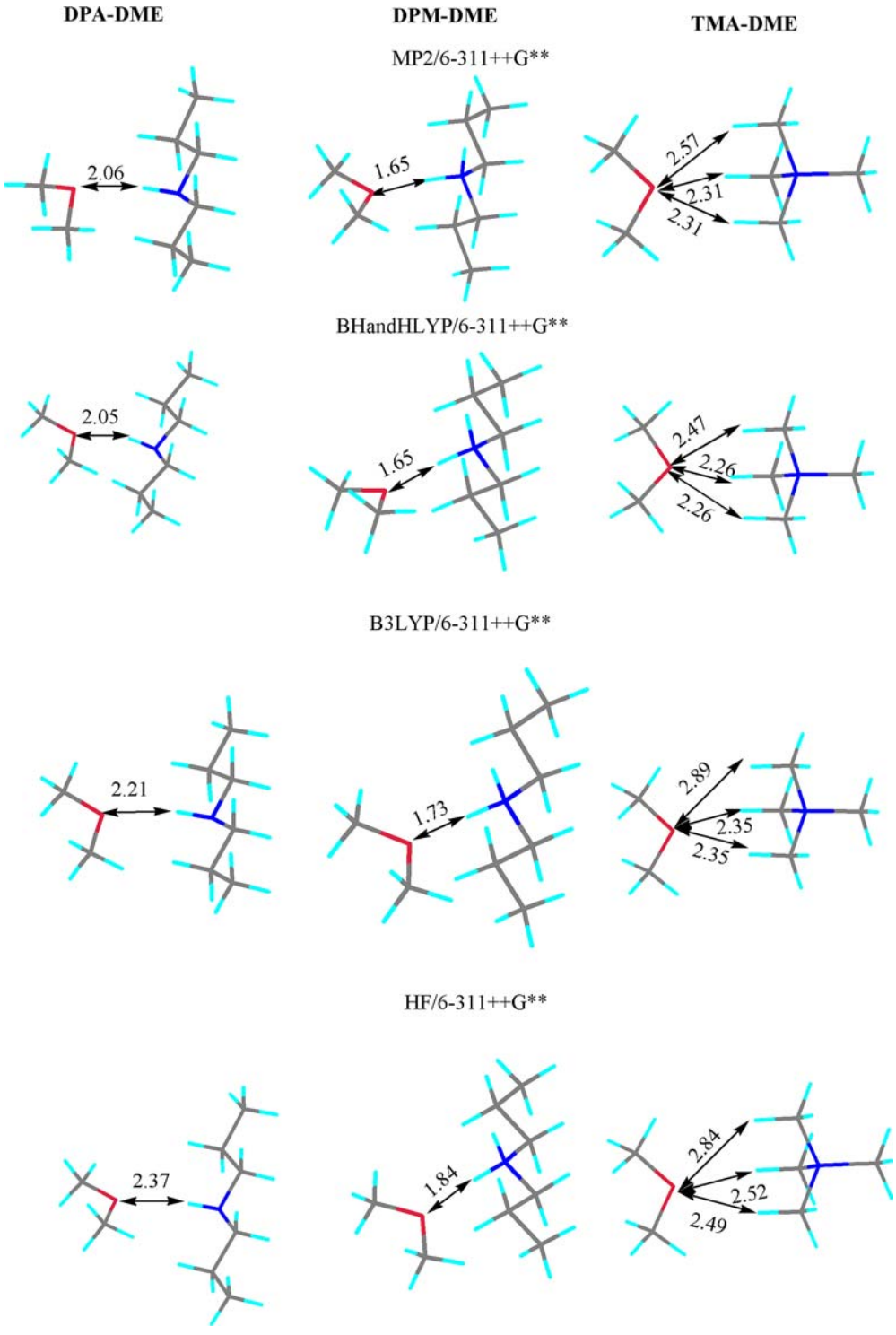

Fig. 2 Optimized structures of model complexes at different theoretical levels

correlation term, which is missing in HF theory. The B3LYP functional is known to be unreliable for systems where dispersion energy is important, which is the main part of correlation stabilization [30]. In the case of the charged DPM–DME and TMA–DME complexes, where electrostatic interactions contribute most to the binding energy, the HF and B3LYP models perform better, as seen from Table 1. The difference between MP2 and HF and B3LYP optimized geometries is less: 0.18 and 0.06 Å, respectively, for the DPM-DME complex (O–H distance). A similar situation is observed for the TMA–DME complex, where the longest O–H distances in MP2 and HF and B3LYP optimized geometries differ by 0.27 and 0.32 Å, respectively. As seen from Table 1, TMA–DME is stabilized mostly by electrostatic interactions and the correlation stabilization represents about 30% of the total stabilization energy at the MP2/6-311 + + G** level, similar to that in the DPM–DME complex. As seen from Table 2, the most important contribution to the stabilization of the TMA–DME complex is the electrostatic interaction.

As seen from Table 1 and Fig. 2, the BHandHLYP functional reproduces the MP2 interaction energies of charged and neutral complexes well. Moreover, the BHandHLYP optimized geometries of the neutral and charged complexes are very close to the MP2 optimized ones. It has been shown earlier that the BHandHLYP functional reproduces MP2 geometries and binding energies of weakly bounded complexes well [31, 32].

The pseudorotoxane-type complex between DB24C8 and *n*-butylammonium (DB24C8–DBM) was first synthesized and characterized by Stoddart et al. [8]. The gas phase optimized geometry at the BHandHLYP/6-311 + + G** level is shown in Fig. 3. The optimized geometry of the complex qualitatively reproduces the X-ray structure of the DB24C8–DBM cation with a PF_6^- counterion, where NH-O hydrogen bonds are formed by phenol and ether oxygens, respectively. Figure 3 shows the overall optimized geometry and selected calculated and experimental distances [8]. The differences observed between the X-ray structure and the gas phase optimized geometry could be related to the fact that the lowest energy conformers are different in the solid and gas phases. Thus, the geometry optimization of the conformer corresponding to the X-ray structure [8] at BHandHLYP/6-311 + + G** makes the structure 2 kcal mol^{-1} less stable than the lowest energy conformer located with the conformational search program. As seen from Fig. 3, the *n*-butylammonium cation is bonded to the crown ether ring by two NH–O and one NCH–O hydrogen bonds, similar to those found for the solid state [8]. The hydrogen-bond lengths in the DB24C8–DBM complex, both experimental and theoretical are significantly shorter than those of the model complex DPM–DME, which might reflect steric hindrance in the pseudorotoxane compared to the model complexes.

The binding energies of the DB24C8–DBM complexes at the BHandHLYP/6-311 + G** and MP2/6-311 + G**//BHandHLYP/6-311 + G** levels are shown in Table 1. Both methods give binding energies in the range of −41 to −43 kcal mol^{-1}. Similar to the DPM–DME complex, the correlation stabilization represents 20–25% of total binding energy. One can estimate the contributions of different types of bonding to the stabilization energy of the DB24C8–DBM complex. Two NH–O hydrogen bonds in DB24C8–DBM will contribute to the binding energy as the double stabilization energy of the DPM–DME complex giving a sum of −30.96 kcal mol^{-1}. The total binding energy of the DB24C8–DBM complex reaches −41.1 kcal mol^{-1} at theBHandHLYP/6-311 + + G** level. The rest of the binding energy can be attributed to NCH–O hydrogen bonding. The model TMA–DME complex has a binding energy of −9.21 kcal mol^{-1} at the BHandHLYP/6-311 + + G** level giving a total binding energy of −40.17 kcal mol^{-1}, very close to the binding energy of the DB24C8–DBM complexes. Therefore, the calculations show that the DB24C8–DBM complex is stabilized by two NH–O and one NCH–O hydrogen bonds, in line with the X-ray diffraction data of the DB24C8–DBM complex [8]. A small difference of 1 kcal mol^{-1} can be attributed to the additional weak NCH–O interactions. Thus, the four NCH–O distances in the DB24C8–DBM complex are 2.21, 2.39, 2.44 and 2.47 Å (Fig. 2). The shortest bond contributes most to the additional stabilization, while the longer ones contribute the rest. A similar picture is observed for the MP2 model. Two NH–O and one NCH–O bonds give −42.5 kcal mol^{-1}, while the total MP2/6-311 + + G** binding energy is −43.1 kcal mol^{-1}. The determination of the gas phase binding energy in the c–$C_6H_{11}NH_3^+$ −18-crown-6 complex using a proton-transfer experiment in a high pressure mass-spectrometer gave −46 ± 4 kcal mol^{-1} [14]. The complex is stabilized by three ionic hydrogen bonds similar to those in DB24C8–DBM. A theoretical estimation of the binding energy using the additivity scheme gives −48.0 and −46.4 kcal mol^{-1} for the MP2/6-311 + + G** and BHandHLYP/6-311 + + G** levels of theory, respectively, which is in excellent agreement with the experiment.

When analyzing the HF energy contributions to the binding energy using the Kitaura–Morokuma energy-decomposition scheme (Table 2) one can see that the electrostatic interactions in the DB24C8–DBM complex correspond to the sum of electrostatic interactions in the TMA–DME complex and two DPM–DME complexes with an error of 0.67 kcal mol^{-1}. A similar situation holds for the polarization and charge transfer contributions. In the case of the exchange repulsion, however, the sum of two exchange repulsions of DPM–DME and TMA-DME (43.6 kcal mol^{-1}) is larger than the exchange repulsion in the DB24C8–DBM complex (33.0 kcal mol^{-1}), which can be attributed to large H-O distances in DB24C8–DBM compared to DPM–DME, causing less electron repulsion in the former.

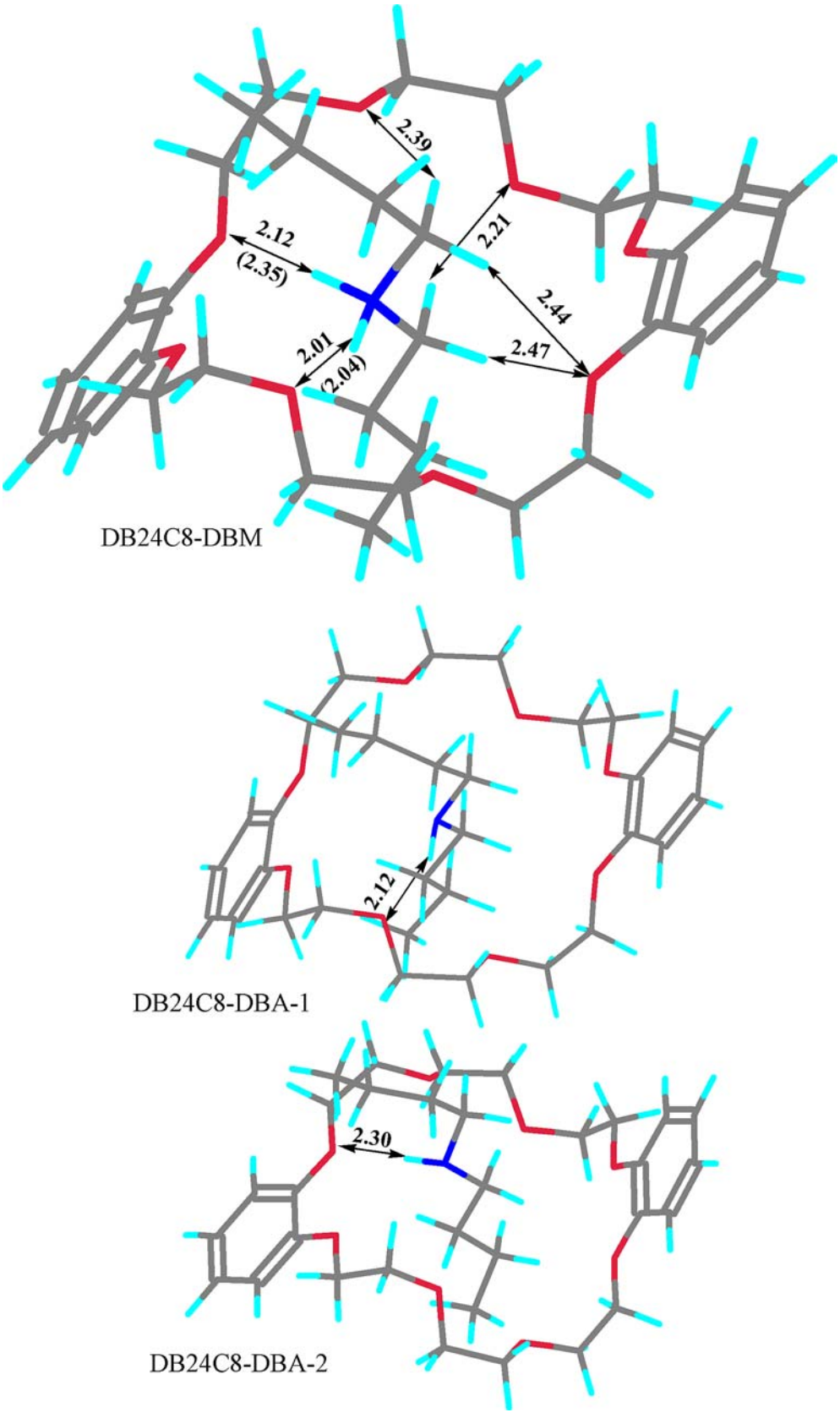

Fig. 3 BHandHlyp/6-311 + + G** optimized structures of DB24C8–DBM, DB24C8–DBA-1 and DB24C8–DBA-2 complexes. Experimental bond lengths are in brackets [8]

The deprotonation of the DB24C8–DBM complex results in the disassembling of pseudorotoxane DB24C8–DBM [8]. The deprotonation gives two different conformers (Fig. 3) depending on the proton abstracted. All levels of theory predict DB24C8–DBA-1 and DB24C8–DBA-2 complexes to be metastable after

taking BSSE into account, with positive binding energies and very similar stabilities. The only contribution to the binding energy is an NH–O hydrogen bond. The binding energies of DPA–DME at the MP2 and BHandHLYP levels are of −2.76 and −2.77 kcal mol^{-1}, although small but negative. As mentioned above, correlation stabilization represents the most important contribution to their stability. As seen from Table 1, the correlation stabilization of the DB24C8–DBA-1 and DB24C8–DBA-2 complexes is significantly more negative than for DPA–DME; −12.66 and −13.26 kcal mol^{-1} at the MP2/6-311++G** level of theory. Therefore, the destabilization of DB24C8–DBA-1 and DB24C8–DBA-2 complexes is related to the HF energy contribution. Table 2 shows the Kitaura–Morokuma energy decomposition. The electrostatic interactions in DB24C8–DBA complexes are almost twice as negative as in DPA–DME, revealing additional interactions apart from NH–O hydrogen bonding in the DB24C8–DBA complexes. The same situation holds for the polarization and especially charge transfer energies, which becomes as important as electrostatic stabilization for DB24C8–DBA complexes. According to the Kitaura–Morokuma energy-decomposition analysis, exchange repulsion is the main factor destabilizing the neutral complexes DB24C8–DBA-1 and DB24C8–DBA-2. Although the exchange repulsion is stronger for the charged DB24C8–DBM complex because of their more compact structure, the additional electrostatic stabilization overcompensates the increase in exchange repulsion.

The association constant of the DB24C8–DBM complex depends strongly on the polarity of the solvent [8], decreasing with the solvent dielectric constant and thus sustaining the hypothesis of the predominance of electrostatic interactions in the stabilization of DB24C8–DBM. Table 3 shows the calculated binding and the free Gibbs binding energies of the DB24C8–DBM complex in different solvents. As seen, the binding energies decrease with solvent polarity, in agreement with the available experimental data. When comparing the experimental and theoretical free Gibbs binding energies, one finds reasonable agreement between theory and experiment (Table 3). Highly polar solvents impede while those with low dielectric constant allow complex formation. The observed agreement between the experiment and theory validates the conclusions on the nature of intermolecular interactions obtained using the present theoretical model.

Table 3 BHandHLYP/6-311++G** binding energies (ΔE), the free Gibbs binding energies (ΔG) at 298 K of DB24C8–DBM complex in different solvents (kcal mol^{-1})

Solvent	ΔE	ΔG	ϵ[a]
Water	−6.1	4.9	78.4
Acetonitryl	−10.3	−0.7 (−3.6)[b]	35.9
Acetone	−11.7	−0.7 (−3.5)[b]	20.6
Chloroform	−18.1	−7.1 (−6.0)	4.81
Methylenechloride	−14.1	−3.1	8.9

[a]Solvent dielectric constants taken from Ref. [33]
[b]Experimental data from Ref. [8]

Conclusions

The most important contributions to the binding energy of dibenzo-24-crown-8—secondary ammonium pseudorotoxanes are electrostatic interactions, polarization energy and charge transfer. Correlation stabilization at the MP2 level of theory represents 20–25% of the total stabilization energy. The BHandHLYP functional produces geometries and interaction energies closest to the MP2 model while the B3LYP and HF methods are less satisfactory. According to our calculations, the pseudorotoxane is stabilized by two NH–O and one NCH–O hydrogen bonds. The latter comprises about 25% of the total interaction energy, giving a total binding energy of −41.2 kcal mol^{-1} at the BHandHLYP/6-311++G** level. Available experimental data on crown ether–ammonium complex stability agree very well with the theoretical calculations. Deprotonation reduces the binding energy by some 50 kcal mol^{-1}, giving the metastable complexes DB24C8–DBA-1 or DB24C8–DBA-2, which will dissociate to give free crown ether and *n*-dibutylamine because of strong exchange repulsion.

Acknowledgements This research was carried out with the support of grant IX-100902/14 from DGAPA.

References

1. Pedersen CJ (1967) J Am Chem Soc 89:7017–7036
2. Cram DJ, Cram JM (1974) Science 183:803–809
3. Cram DJ, Cram JM (1978) Acc Chem Res 11:8–14
4. Peczuh MW, Hamilton AD (2000) Chem Rev 100:2479–2494
5. Reinhoudt DN (1988) J Coord Chem 18:21–43
6. Koike T, Takashige M, Kimura E, Fujioka H, Shiro M (1996) Chem Eur J 2:617–623
7. Aoki S, Kimura E (2000) J Am Chem Soc 122:4542–4548
8. Ashton PR, Campbell PJ, Chrystal EJT, Glink PT, Menzer S, Philp D, Spencer N, Stoddart JF, Tasker PA, Williams DJ (1995) Angew Chem Int Ed Engl 34:1865–1869
9. Kolchinski AG, Busch DH, Alcock NW (1995) J Chem Soc Chem Commun 12:1289–1291
10. Ashton PR, Ballardini R, Balzani V, Gomez-Lopez M, Lawrence SE, Martinez-Diaz MV, Montalti M, Piersanti A, Prodi L, Stoddart JF, Williams DJ (1997) J Am Chem Soc 119:10641–10651
11. Martinez-Diaz MV, Spencer N, Stoddart JF (1997) Angew Chem Int Ed Engl 36:1904–1907
12. Ashton PR, Ballardini R, Balzani V, Baxter I, Credi A, Fyfe MCT, Gandolfi MT, Gomez-Lopez M, Martinez-Díaz MV, Piersanti A, Spencer N, Stoddart JF, Venturi M, White AJP, Williams DJ (1998) J Am Chem Soc 120:11932–11942
13. Cantrill SJ, Pease AR, Stoddart JF (2000) J Chem Soc Dalton Trans 21:3715–3734
14. Moet-Ner M (1983) J Am Chem Soc 105:4912–4915
15. Ha YL, Chakraborty AK (1992) J Phys Chem 96:6410–6417
16. Choe JI, Chang SK, Ham SW, Nanbu S, Aoyagi M (2001) Bull Korean Chem Soc 22:1248–1254

17. Lazar A, Angyan JG, Hollosi M, Huszthy P, Surjan PR (2002) Chirality 15:377–385
18. Yang K, Duck-Kang K, Hee-Park Y, Sun-Koo I, Lee I (2003) Chem Phys Lett 239–243
19. Frankfort L, Sohlberg K (2003) J Mol Struct (Theochem) 621:253–260
20. Raymo FM, Bartberger MD, Houk KN, Stoddart JF (2001) J Am Chem Soc 123:9264–9267
21. Titan Version 1.05. (1999) Wavefunction Inc, Schrodinger Inc
22. Boys SF, Bernardi F (1970) Mol Phys 19:553–566
23. Tannor DJ, Marten B, Murphy R, Friesner RA, Sitkoff D, Nicholls A, Ringnalda M, Goddard WA, Honig B (1994) J Am Chem Soc 116:11875–11882
24. Marten B, Kim K, Cortis C, Friesner RA, Murphy RB, Ringnalda M, Sitkoff D, Honig B (1996) J Phys Chem 100:11775–11778
25. Jaguar 5.5 (2003) Schrodinger, LLC, Portland, Oregon
26. Frisch MJ, Trucks GW, Schlegel HB, Scuseria GE, Robb MA, Cheeseman JR, Montgomery JA, Vreven T, Kudin KN, Burant JC, Millam JM, Iyengar SS, Tomasi J, Barone V, Mennucci B, Cossi M, Scalmani G, Rega N, Petersson GA, Nakatsuji H, Hada M, Ehara M, Toyota K, Fukuda R, Hasegawa J, Ishida M, Nakajima T, Honda Y, Kitao O, Nakai H, Klene M, Li X, Knox JE, Hratchian HP, Cross JB, Adamo C, Jaramillo J, Gomperts R, Stratmann RE, Yazyev O, Austin AJ, Cammi R, Pomelli C, Ochterski JW, Ayala PY, Morokuma K, Voth GA, Salvador P, Dannenberg JJ, Zakrzewski VG, Dapprich S, Daniels AD, Strain MC, Farkas O, Malick DK, Rabuck AD, Raghavachari K, Foresman JB, Ortiz JV, Cui Q, Baboul AG, Clifford S, Cioslowski J, Stefanov BB, Liu G, Liashenko A, Piskorz P, Komaromi I, Martin RL, Fox DJ, Keith T, Al-Laham MA, Peng CY, Nanayakkara A, Challacombe M, Gill PMW, Johnson B, Chen W, Wong MW, Gonzalez C, Pople JA (2003) Gaussian 03, Revision B.04. Gaussian Inc, Pittsburgh PA
27. Kitaura K, Morokuma K (1976) Int J Quantum Chem 10: 325–340
28. Schmidt MW, Baldridge KK, Boatz JA, Elbert ST, Gordon MS, Jensen JH, Koseki S, Matsunaga N, Nguyen KA, Su S, Windus TL, Dupuis M, Montgomery JA (1993) J Comput Chem 14:1347–1363
29. Meot-Ner M (2005) Chem Rev 105:213–284
30. Chalasinski G, Szczesniak MM (2000) Chem Rev 100:4227–4252
31. Ruiz E, Salahub DR, Vela A (1995) J Am Chem Soc 117:1141–1142
32. Romero C, Fomina L, Fomine S (2005) Int J Quant Chem (in press)
33. Reichardt (1988) Solvents and Solvent effects in Organic Chemistry. VCH Weinheim, Germany